

## Synthesis and Fundamental Properties of Stable $\text{Ph}_3\text{SnSiH}_3$ and $\text{Ph}_3\text{SnGeH}_3$ Hydrides: Model Compounds for the Design of Si–Ge–Sn Photonic Alloys

Jesse B. Tice,\* Andrew V. G. Chizmeshya, Thomas L. Groy, and John Kouvetakis

Department of Chemistry and Biochemistry, Arizona State University, Tempe, Arizona 85287

Received March 30, 2009

The compounds  $\text{Ph}_3\text{SnSiH}_3$  and  $\text{Ph}_3\text{SnGeH}_3$  ( $\text{Ph} = \text{C}_6\text{H}_5$ ) have been synthesized as colorless solids containing  $\text{Sn}-\text{MH}_3$  ( $\text{M} = \text{Si}, \text{Ge}$ ) moieties that are stable in air despite the presence of multiple and highly reactive  $\text{Si}-\text{H}$  and  $\text{Ge}-\text{H}$  bonds. These molecules are of interest since they represent potential model compounds for the design of new classes of IR semiconductors in the Si–Ge–Sn system. Their unexpected stability and high solubility also makes them a safe, convenient, and potentially useful delivery source of  $-\text{SiH}_3$  and  $-\text{GeH}_3$  ligands in molecular synthesis. The structure and composition of both compounds has been determined by chemical analysis and a range of spectroscopic methods including multinuclear NMR. Single crystal X-ray structures were determined and indicated that both compounds condense in a  $Z = 2$  triclinic ( $P\bar{1}$ ) space group with lattice parameters ( $a = 9.7754(4) \text{ \AA}$ ,  $b = 9.8008(4) \text{ \AA}$ ,  $c = 10.4093(5) \text{ \AA}$ ,  $\alpha = 73.35(10)^\circ$ ,  $\beta = 65.39(10)^\circ$ ,  $\gamma = 73.18(10)^\circ$ ) for  $\text{Ph}_3\text{SnSiH}_3$  and ( $a = 9.7927(2) \text{ \AA}$ ,  $b = 9.8005(2) \text{ \AA}$ ,  $c = 10.4224(2) \text{ \AA}$ ,  $\alpha = 74.01(3)^\circ$ ,  $\beta = 65.48(3)^\circ$ ,  $\gamma = 73.43(3)^\circ$ ) for  $\text{Ph}_3\text{SnGeH}_3$ . First principles density functional theory simulations are used to corroborate the molecular structures of  $\text{Ph}_3\text{SnSiH}_3$  and  $\text{Ph}_3\text{SnGeH}_3$ , gain valuable insight into the relative stability of the two compounds, and provide correlations between the Si–Sn and Ge–Sn bonds in the molecules and those in tetrahedral Si–Ge–Sn solids.

### Introduction

Recently, we reported the fabrication of new  $\text{Ge}_{1-x}\text{Sn}_x$  binary alloys with Sn contents up to 20 at.% grown directly on Si via reactions of  $\text{SnD}_4$  and  $\text{Ge}_2\text{H}_6$ .<sup>1</sup> Si incorporation into these materials to form  $\text{Si}_{1-x-y}\text{Ge}_x\text{Sn}_y$  ( $\text{Sn} < 12\%$  at. %) ternaries was subsequently achieved using new silylgermanes ( $\text{GeH}_3$ )<sub>x $\text{SiH}_{4-x}$  as the source of Si and Ge.<sup>2,3</sup> The ternary materials exhibit independently tunable bandgaps and lattice parameters thereby making it possible to envision entirely new families of optoelectronic devices ranging from communication applications (modulators to quantum cascade lasers) to sustainable energy systems such as high efficiency photovoltaics. The emergence of the SiGeSn system have also led to the development of  $\text{Si}_{1-x}\text{Sn}_x$  alloys as a logical offshoot.<sup>4</sup> The latter cover a wide range of band-gaps that are predicted to become direct for  $x = 0.30$ – $0.50$  leading to additional applications in high performance IR systems.<sup>1,5</sup></sub>

To date, a limited number of  $\text{Si}_{1-x}\text{Sn}_x$  samples within the range of  $0.10 < x < 0.25$  has been demonstrated via reactions of  $\text{SnD}_4$  and trisilane, while the analogous growth of  $\text{Ge}_{1-x}\text{Sn}_x$  has been limited to Sn fractions of less than 20 at. %. This suggests that the fabrication of higher Sn contents approaching 50% in the binaries may require the development of alternate lower temperature routes ideally involving single source precursors with direct M–Sn bonds ( $\text{M} = \text{Si}, \text{Ge}$ ). Such compounds are likely to be more reactive and able to furnish the entire molecular core intact to the crystal lattice of the product. In this regard, pure heteroatom stannyl-hydrides  $\text{H}_3\text{MSnH}_3$  with preformed Sn–M bonds represent, in principle, the most suitable precursors for this application. Prior work has established that access to these molecules is vitiated by their inherent instability with respect to decomposition into  $\text{MH}_4$ , elemental Sn, and  $\text{H}_2$ .<sup>6</sup> One possible solution to this problem would be to increase the molecular stability of the tin functionality in the compound by replacing one or more of the weak Sn–H bonds with suitable organic groups such as phenyls ( $\text{Ph} = \text{C}_6\text{H}_5$ ). Particularly attractive targets include the  $(\text{H}_{3-x}\text{Ph}_x)\text{SnSiH}_3$  and  $(\text{H}_{3-x}\text{Ph}_x)\text{SnGeH}_3$  series of molecules since these are likely to thermally eliminate the phenyl and the H ligands as benzene byproducts leading to the delivery of the desired

\*To whom correspondence should be addressed. E-mail: jesse.tice@asu.edu.

(1) Bauer, M.; Taraci, J.; Tolle, J.; Chizmeshya, A. V. G.; Zollner, S.; Smith, D. J.; Menendez, J.; Hu, C.; Kouvetakis, J. *J. Appl. Phys. Lett.* **2002**, 81 (16), 2992–2994.

(2) Fang, Y.-Y.; Xie, J.; Tolle, J.; Roucka, R.; D'Costa, V. R.; Chizmeshya, A. V. G.; Menendez, J.; Kouvetakis, J. *J. Am. Chem. Soc.* **2008**, 130(47), 16095–16102.

(3) Kouvetakis, J.; Menendez, J.; Chizmeshya, A. V. G. *Ann. Rev. Mat. Res.* **2006**, 36, 497–554.

(4) Tolle, J.; Chizmeshya, A. V. G.; Fang, Y.-Y.; Kouvetakis, J.; D'Costa, V. R.; Hu, C.-W.; Menendez, J.; Tsong, I. S. T. *J. Appl. Phys. Lett.* **2006**, 89 (23), 231924/1–231924/3.

(5) Soref, R. *IEEE J. Sel. Top. Quantum Electron.* **2006**, 12, 1678.

(6) Wiberg, E.; Amberger, E.; Cambensi, H. Z. *Anorg. Allg. Chem.* **1967**, 351(3–4), 164–179.

Si–Sn and Ge–Sn composition in the solid. In our prior work we have successfully applied a similar strategy to produce  $\text{Ge}_{1-x}\text{Sn}_x$  alloys using  $\text{PhSnD}_3$ , as a viable Sn source in the deposition of thin films via elimination of benzene according to the following reaction:  $\text{PhSnD}_3 \rightarrow \text{D}_2 + \text{Ph(D)} + \text{Sn}$ .

Historically, the creation of molecules containing Si–Sn bonds and metal hydride functionalities  $\text{MH}_x$  (where  $x = 1-3$ ) has proven to be very difficult as evidenced by the paucity of references in the literature concerning their syntheses and characterizations. In this regard, the possible formation of  $\text{Me}_3\text{SnSiH}_3$  ( $\text{Me} = \text{CH}_3$ ) and  $(\text{Me}_3\text{Sn})_3\text{SiH}$  was reported on the basis of  $^1\text{H}$  NMR data.<sup>8</sup> However no product yields were given since the materials were highly sensitive to light and presumably could not be readily isolated for further analysis. In subsequent work, the presence of trace amounts of  $\text{Me}_3\text{SnSiH}_3$  was observed as a byproduct during the synthesis of  $\text{Me}_3\text{SnSiF}_3$  from a reaction of  $\text{Me}_3\text{SnH}$  and  $\text{Si}_2\text{F}_6$ .<sup>9</sup> We note that further efforts to isolate and characterize  $\text{Me}_3\text{SnSiF}_3$  in viable yields have not been reported, and its application as a source of pure Si–Sn will likely be hampered by the presence of thermally reactive  $\text{CH}_3$  ligands, potentially leading to C contamination. Related compounds with single Si–H bonds such as  $\text{HSi}(\text{SnMe}_3)_3$  and  $\text{Bu}_3\text{SnSi}(\text{H})\text{Me}_2$  ( $\text{Bu} = n\text{-C}_4\text{H}_9$ ) were prepared and characterized by physicochemical methods; however, their molecular structures were not reported.<sup>10,11</sup> In more recent work, the successive buildup of  $\text{SiH}_3$  groups around a central tin atom was purportedly achieved using reactions of  $\text{NaSiH}_{3-n}(\text{SiH}_3)_n$  with  $\text{SnH}_4$  to yield silyl-substituted sodium stannides with a proposed formula of  $\text{NaSnH}_{3-n}(\text{SiH}_3)_n$ .<sup>12</sup> These materials were found to be marginally stable in glyme solutions on a time scale sufficient to obtain NMR data but were never isolated in pure form. Finally, a more stable series of hydrido-substituted stannylsilanes including the  $\text{HMe}_2\text{SiSnPh}_2\text{Me}$ ,  $\text{HSiR}_2\text{Bu}_2\text{SnCl}$  ( $\text{R} = i\text{-prop, } t\text{-but}$ ), and  $\text{H-SiR}'_2\text{-R}_2\text{Sn-Z}$  ( $\text{R}' = \text{Me, } i\text{-prop, } t\text{-but, } \text{R} = \text{Me, } t\text{-but, and } \text{Z} = \text{H, Me}$ ) have also been reported.<sup>13,14</sup>

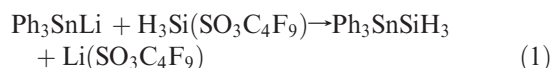
While, to the best of our knowledge, the above examples represent the only extant organotin silanes in the literature, instances of the analogous organotin germanes containing Ge–H bonds are even rarer. For example  $\text{Me}_3\text{SnGeH}_3$  was prepared in minor amounts and was only characterized by  $^1\text{H}$  NMR.<sup>15</sup> Attempts to prepare the ethyl derivative  $\text{Me}_3\text{SnGeEt}_2\text{H}$  ( $\text{Et} = \text{C}_2\text{H}_5$ ) and the closely related

$\text{Et}_3\text{SnGe}(\text{C}_6\text{F}_5)_2\text{H}$  analogue were also reported exclusively on the basis of FTIR characterizations.<sup>16,17</sup> On the basis of the aforementioned studies it appears that Sn–Si or Sn–Ge metalorganics containing  $\text{SiH}_x$  and  $\text{GeH}_x$  moieties are relatively unstable or inconclusively characterized, particularly when multiple hydride bonds are present.

In this paper, we report the synthesis of the simple and remarkably robust Si–Sn and Ge–Sn compounds with compositions  $\text{Ph}_3\text{SnSiH}_3$  and  $\text{Ph}_3\text{SnGeH}_3$ . These represent the first example of molecules within this class containing intact silyl and germyl groups that are stable in air. Also, these compounds can be obtained in single crystalline form thereby enabling their unequivocal identification by X-ray diffraction (XRD) determination of their molecular structures. Theoretical simulations were used to corroborate the molecular structures, elucidate their intrinsic thermochemical properties, and predict their relative stability in relation to both standard states and hypothetical SiSn and GeSn compounds.

## Results and Discussion

The preparation of  $\text{Ph}_3\text{SnSiH}_3$  was initially explored using metathesis reactions involving  $\text{H}_3\text{Si}(\text{SO}_3\text{CF}_3)$  and common alkali silanide salts such as  $\text{KSiH}_3$ . The main drawback with the use of the latter in such nucleophilic addition reactions was the limited stability of the salt in tetrahydrofuran (THF) solutions resulting in its decomposition into higher order silanides and unstable Si–H polymers. In the case of the triflate,  $\text{H}_3\text{Si}(\text{SO}_3\text{CF}_3)$ , the primary limitation precluding its successful use is the rapid decomposition of the compound above  $-10^\circ\text{C}$  to form highly explosive  $\text{SiH}_4$  byproducts. In view of these difficulties, we next employed  $\text{H}_3\text{Si}(\text{SO}_3\text{C}_4\text{F}_9)$  (a butane analogue of the silyl triflate) which as shown below, represents a highly stable and therefore more practical source of  $\text{SiH}_3$  compared to both  $\text{H}_3\text{Si}(\text{SO}_3\text{CF}_3)$  and  $\text{KSiH}_3$ . Under optimal conditions the stoichiometric reaction of  $\text{H}_3\text{Si}(\text{SO}_3\text{C}_4\text{F}_9)$ <sup>18</sup> and  $\text{Ph}_3\text{SnLi}$ <sup>19</sup> readily produced the target compound as a crystalline solid via elimination of  $\text{Li}(\text{SO}_3\text{C}_4\text{F}_9)$  (see eq 1):



A minor limitation associated with the use of the  $\text{H}_3\text{Si}(\text{SO}_3\text{C}_4\text{F}_9)$  was its propensity to react slowly with the THF solvent to form polymeric byproducts leading to its gradual degradation under prolonged reaction times. This difficulty was overcome by using stringent reaction conditions involving the slow addition of  $\text{H}_3\text{Si}(\text{SO}_3\text{C}_4\text{F}_9)$  to a THF solution of  $\text{Ph}_3\text{SnLi}$  at  $-35^\circ\text{C}$  followed by stirring the resulting suspension at  $22^\circ\text{C}$  for 1 h. This led to the formation of the desired product in  $\sim 40\%$  yield. We note that our attempts to produce  $\text{Ph}_3\text{SnSiH}_3$  using solutions of  $\text{Ph}_3\text{SnLi}$  in solvents other than THF (such as diethyl ether and glymes) produced large amounts of  $\text{SiH}_4$  resulting from the decomposition of the  $\text{H}_3\text{Si}(\text{SO}_3\text{C}_4\text{F}_9)$  starting material. Additionally, we

(7) Taraci, J.; Zollner, S.; McCartney, M. R.; Menendez, J.; Santana-Aranda, M. A.; Smith, D. J.; Haaland, A.; Tutukin, A. V.; Gundersen, G.; Wolf, G.; Menendez, J.; Kouvetakis, J. *J. Am. Chem. Soc.* **2001**, *123*(44), 10980–10987.

(8) Amberger, E.; Muehlhofer, E. *J. Organomet. Chem.* **1968**, *12*(1), 55–62.

(9) D'Errico, J. J.; Sharp, K. G. *J. Chem. Soc., Dalton Trans: Inorg. Chem.* **1989**, *9*, 1879–18781.

(10) Heyn, R. H.; Tilley, T. D. *Inorg. Chem.* **1990**, *29*(20), 4051–4055.

(11) Lahournere, J. C.; Valade, J. C. *R. Soc. Acad. Sci., Ser. C: Sci. Chim.* **1970**, *270*(25), 2080–2082.

(12) Lobreyer, T.; Sundermeyer, W.; Oberhammer, H. *Chem. Ber.* **1994**, *127*(11), 2111–2115.

(13) Uhlig, F.; Kayser, C.; Klassen, R.; Hermann, U.; Brecker, L.; Schuermann, M.; Ruhland-Senge, K.; Englich, U. *Z. Natur. B: Chem. Sci.* **1999**, *54*(2), 278–287.

(14) Englich, U.; Prass, I.; Schollmeier, T.; Uhlig, F. *Monatsh. Chem.* **2001**, *627*(3), 453–457.

(15) Angus, P. C.; Stobart, S. R. *J. Chem. Soc., Dalton Trans: Inorg. Chem.* **1973**, No. 21, 2374–2380.

(16) Bravo-Ahivotovskii, D.; Biltueva, I.; Vyazankina, O.; Vyazankin, N. *Izv. Akad. Nauk SSSR Ser. Khim.* **1985**, 1214.

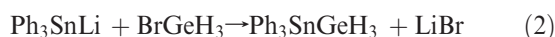
(17) Bochkarev, M.; Maiorova, L.; Razuvaev, G. *Zh. Obshch. Khim.* **1980**, *50*, 903–907.

(18) Tamborski, C.; Ford, F. E.; Soloski, E. J. *J. Org. Chem.* **1963**, *28*, 181–184.

(19) Lobreyer, T.; Oeler, J.; Sundermeyer, W. *Chem. Ber.* **1991**, *124*(11), 2405–2410.

observed no product formation when an excess of either  $\text{Ph}_3\text{SnLi}$  or  $\text{H}_3\text{Si}(\text{SO}_3\text{C}_4\text{F}_9)$  was employed indicating that any non-stoichiometric mixture increases the decomposition rate of both reactants. Collectively the above results indicate that the metathesis mechanism leading to the desired product is only operative over a very narrow range of reaction conditions, most notably temperature, solvent type, and reactant ratio. The  $\text{Ph}_3\text{SnSiH}_3$  product was separated and isolated from the main reaction byproduct  $\text{Li}(\text{SO}_3\text{C}_4\text{F}_9)$  and a side reaction impurity  $\text{Ph}_4\text{Sn}$  as a colorless solid exhibiting a sharp melting point of 86 °C.

The  $\text{GeH}_3$  analogue [ $\text{Ph}_3\text{SnGeH}_3$ ] of the above  $\text{Ph}_3\text{SnSiH}_3$  compound was synthesized via a stoichiometric combination of freshly prepared  $\text{BrGeH}_3$  and  $\text{Ph}_3\text{SnLi}$  dissolved in THF (eq 2):



The reaction is stirred for 15 h to produce  $\text{Ph}_3\text{SnGeH}_3$  (50% yield) which was isolated from the main reaction byproduct  $\text{LiBr}$  and a side reaction impurity  $\text{Ph}_4\text{Sn}$  as a colorless solid exhibiting a sharp melting point of 82 °C. Note that shorter reaction times (3–5 h) led to minimal amounts of product while longer times did not enhance the overall yield.

Single crystals of the  $\text{Ph}_3\text{SnSiH}_3$  and  $\text{Ph}_3\text{SnGeH}_3$  were grown from a hexane solution of the compounds and subsequently used to perform a complete characterization by XRD, multinuclear NMR, IR spectroscopy, combustion analysis, and mass spectrometry. Collectively, the results indicate that the molecules are isostructural and consist of  $\text{MH}_3$  and  $\text{SnPh}_3$  groups connected with single  $\text{Sn}-\text{M}$  bonds. This close correspondence in molecular architecture affords a straightforward comparison of the structural and spectroscopic properties as summarized in Table 1. Accordingly, here we provide a detailed interpretation of the spectroscopic data for  $\text{Ph}_3\text{SnSiH}_3$  and refer the reader to Table 1 and the experimental section for further details regarding the  $\text{Ph}_3\text{SnGeH}_3$  analogue.

The  $^1\text{H}$  NMR data of  $\text{Ph}_3\text{SnSiH}_3$  revealed a singlet at 3.66 ppm corresponding to the  $\text{SiH}_3$  protons and multiplets at 7–7.5 ppm due to the *ortho*, *meta*, and *para* protons of the Ph group. Satellite peaks induced by the  $^{117/119}\text{Sn}$  nuclei are found to be symmetrically distributed by 56 Hz with respect to their  $^1\text{H}$  singlet, in analogy with those previously reported for  $\text{HSi}(\text{SnMe}_3)_3$  and the  $\text{HSiR}_2\text{SnR}_3$  compounds.<sup>10,14</sup> The corresponding  $^{29}\text{Si}$  satellite peaks were observed at 200 Hz which is a typical value for silyl-germyl hydrides such as  $(\text{GeH}_3)_x\text{SiH}_{4-x}$ .<sup>20</sup> The  $^{119}\text{Sn}$  chemical shift at  $\sim -134$  ppm is characteristic of multiple electron withdrawing phenyls bonded to the Sn atom while the  $^{29}\text{Si}$  shift at  $-106$  ppm is typical for conventional silylgermanes. The 2D  $^1\text{H}$  COSY spectrum indicated no connectivity between the  $\text{Si}-\text{H}$  singlet of the  $\text{SiH}_3$  (3.66 ppm) and the C–H multiplets of the  $\text{SnPh}_3$  (7–7.5 ppm) while the  $^{29}\text{Si}-^1\text{H}$  HMQC spectrum confirms that the Si atom at  $-106$  ppm is bonded exclusively to the protons at 3.66 ppm. Collectively the correlated NMR data corroborate the proposed molecular structure of  $\text{Ph}_3\text{SnSiH}_3$ . The IR spectra showed the characteristic vibrations of the phenyl ring at 3100–3000  $\text{cm}^{-1}$  and

**Table 1.** Summary of Data for  $\text{Ph}_3\text{SnSiH}_3$  and  $\text{Ph}_3\text{SnGeH}_3$

	$\text{Ph}_3\text{SnSiH}_3$	$\text{Ph}_3\text{SnGeH}_3$
NMR Data		
$\delta \text{MH}_3$ (ppm)	3.66	3.50
$\delta^{29}\text{Si}$ (ppm)	−106	
$^{119}\text{Sn}$ (ppm)	−133.6	−134.2
$^1J_{\text{Si}-\text{H}}$ (Hz)	200	
$^2J_{\text{Sn}-\text{H}}$ (Hz)	56	82
FTIR Data		
$\nu \text{C}-\text{H}$ ( $\text{cm}^{-1}$ )	3100–3000	3100–3000
$\nu \text{Si}-\text{H}$ ( $\text{cm}^{-1}$ )	2164, 2130	
$\nu \text{Ge}-\text{H}$ ( $\text{cm}^{-1}$ )		2080, 2045
$\nu \text{Sn}-\text{M}$ ( $\text{cm}^{-1}$ )	315	273
Elemental Analysis		
calculated C and H	56.70, 4.76	50.77, 4.26
observed C and H	56.92, 4.95	50.63, 4.27
Crystal Data		
chemical formula	$\text{C}_{18} \text{H}_{18} \text{Si Sn}$	$\text{C}_{18} \text{H}_{18} \text{Ge Sn}$
formula weight (amu)	381.1	425.7
$D_{\text{CALC}}$ ( $\text{g}/\text{cm}^3$ )	1.486	1.647
volume ( $\text{Å}^3$ )	851.95	857.97
setting/space group	triclinic, $P\bar{1}$	triclinic, $P\bar{1}$
$a$ (Å)	9.7754	9.7927
$b$ (Å)	9.8008	9.8005
$c$ (Å)	10.4093	10.4224
$\alpha$ (deg)	73.347	74.001
$\beta$ (deg)	65.388	65.482
$\gamma$ (deg)	73.184	73.427
$\mu$ ( $\text{cm}^{-1}$ )	1.558	3.195
$Z$	2	2
measurement $T$ (K)	123	123
$R1^a$ (% , all data)	2.51	4.18
$wR2^b$ (% , all data)	6.41	11.01

$$^a R1 = \frac{\sum ||F_o| - |F_c||}{\sum |F_o|} \times 100. \quad ^b wR2 = \frac{\{\sum w(F_o^2 - F_c^2)^2 / \sum w(F_o^2)^2\}^{1/2}}{\times 100}.$$

1950–900  $\text{cm}^{-1}$ , respectively, while the  $\text{SiH}_3$  asymmetric/symmetric stretching modes were observed at 2164/2130  $\text{cm}^{-1}$  as expected. The  $\text{Si}-\text{Sn}$  bond stretch was observed at 314  $\text{cm}^{-1}$  and closely matches the phonon frequencies as measured by Raman in the diamond cubic  $\text{Si}_{1-x}\text{Sn}_x$  alloys. The C and H combustion analysis yielded values essentially identical to those expected (within  $\sim 3\%$ ). The  $\text{Ph}_3\text{SnSiH}_3$  compound decomposes in the mass spectrometer to yield the  $(\text{C}_6\text{H}_5)_3\text{Sn}$  ion as the highest peak at  $\sim 350$  amu indicating that the  $\text{Si}-\text{Sn}$  bond is unstable under these conditions. In contrast, the parent ion of the Ge analogue  $\text{Ph}_3\text{SnGeH}_3$  was seen at 426 amu demonstrating that the intact  $\text{Ge}-\text{Sn}$  bond is stronger than its  $\text{Si}-\text{Sn}$  counterpart. This is also consistent with the bonding properties predicted by quantum chemical calculations of the compounds, as described below.

Crystallographic analyses of  $\text{Ph}_3\text{SnSiH}_3$  and  $\text{Ph}_3\text{SnGeH}_3$  indicates that the compounds are monomeric in the solid state. The  $\text{MH}_3$  ligands are bonded exclusively to the Sn center which in turn is surrounded by three phenyl rings arranged in a “paddle” or propeller-like geometry. Both compounds crystallize in a triclinic unit cell of  $P\bar{1}$  symmetry (see Table 1) containing two identical molecules ( $Z = 2$ ) such as that shown in Figure 1(a) with a thermal ellipsoid model (50% probability). Table 2 contains selected bond distances and angles for the molecular units. The  $\text{Si}-\text{Sn}$  (2.556 Å) and  $\text{Ge}-\text{Sn}$  (2.583 Å) bond distances

(20) Ritter, C. J.; Hu, C.; Chizmeshya, A. V. G.; Tolle, J.; Klewer, D.; Tsong, I. S. T.; Kouvetakis, J. *J. Am. Chem. Soc.* **2005**, *127*(27), 9855–9864.

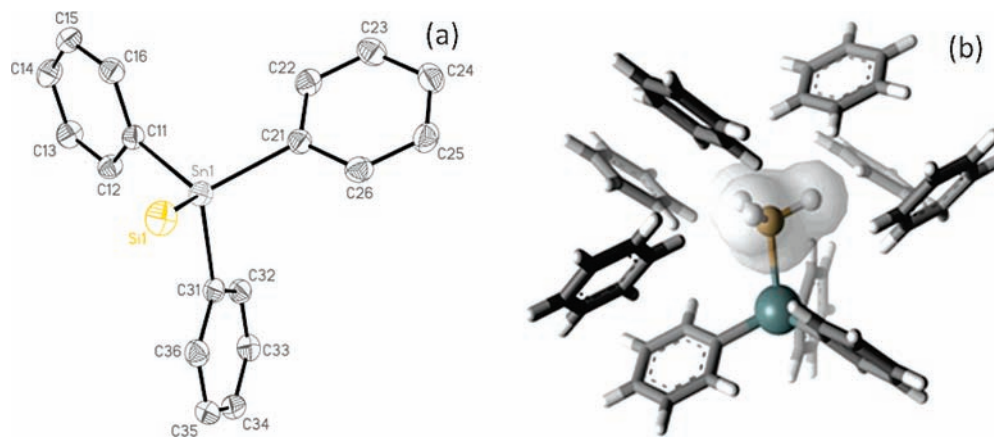


**Figure 1.** (a) Molecular structure of  $\text{Ph}_3\text{SnSiH}_3$ . (b) Coordination of phenyl groups around the  $-\text{SiH}_3$  group within the solid  $\text{Ph}_3\text{SnSiH}_3$  hydride, illustrating a “cage-like” structure around the Si atom with a mean diameter of  $\sim 3$  Å.

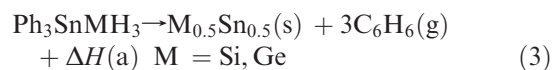
**Table 2.** Selected Inter-Atomic Distances (Å) and Angles (deg) for  $\text{Ph}_3\text{SnSiH}_3$  and  $\text{Ph}_3\text{SnGeH}_3$

$\text{Ph}_3\text{SnSiH}_3$			
Sn(1)–Si(1)	2.556(8)	C(31)–Sn(1)–Si(1)	107.12(7)
Sn(1)–C(11)	2.140(3)	C(21)–Sn(1)–Si(1)	108.15(7)
Sn(1)–C(21)	2.147(3)	Sn(1)–Si(1)–H(1)	114.0(16)
Sn(1)–C(31)	2.145(3)	Sn(1)–Si(1)–H(2)	108.3(15)
Si(1)–H(1)	1.36(4)	Sn(1)–Si(1)–H(3)	110(2)
Si(1)–H(2)	1.36(4)	H(1)–Si(1)–H(2)	105(2)
Si(1)–H(3)	1.32(5)	H(1)–Si(1)–H(3)	115(3)
C(11)–Sn(1)–Si(1)	116.88(7)	H(2)–Si(1)–H(3)	104(3)
$\text{Ph}_3\text{SnGeH}_3$			
Sn(1)–Ge(1)	2.583(7)		
Sn(1)–C(11)	2.149(4)	C(11)–Sn(1)–Ge(1)	115.88(11)
Sn(1)–C(21)	2.142(4)	C(21)–Sn(1)–Ge(1)	107.73(11)
Sn(1)–C(31)	2.145(4)	C(31)–Sn(1)–Ge(1)	106.72(12)

are typical for crystalline compounds containing M–Sn bonds.<sup>21–23</sup> The C–Sn bond distances range from 2.12 to 2.14 Å and are nearly identical to those found in related organometallics of Sn including  $\text{SnPh}_4$ .<sup>24</sup> The inherent internal structure of the phenyl rings remain undistorted as evidenced by the close similarity of *ortho*, *para*, and *meta* bond lengths. The various M–Sn–C and C–Sn–C bond angles range from 107 to 116° revealing a nominal deviation from tetrahedral geometry about the Sn center. A close examination of the packing diagram indicates that the phenyl rings essentially form a protective cage composed of hexagonal panels (paddles) encapsulating the  $\text{MH}_3$  groups in the extended structure as illustrated in Figure 1(b). This arrangement may explain the unusual stability of the solid state samples and their lack of any discernible decomposition in the presence of oxygen and moisture for prolonged time periods of over at least several months.

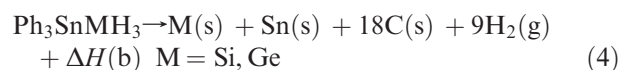
**Simulation Studies of Structure and Stability.** To further corroborate the structural trends discussed above and examine the relative stability of the  $\text{Ph}_3\text{SnSiH}_3$  and  $\text{Ph}_3\text{SnGeH}_3$  compounds we carried out a systematic

density functional theory-based simulation, which allows a comparison of the molecular properties on an equal footing. The simulations focus on the individual molecules rather than the extended solid state structures since the latter are composed of weakly bound monomeric units and a common packing motif. We estimated the relative stability of the title compounds using two decomposition pathways. The first, given by eq 3, describes the hypothetical and complete dissociation of the molecules to form stoichiometric SiSn and GeSn zinc blende phases via elimination of stable benzene byproducts:



Here we consider the most plausible and perhaps simplest decomposition pathway although other mechanisms involving ligand exchange are also possible. To explore this notion we conducted a preliminary experiment in which we heated the bulk solid to temperatures near  $\sim 150$  °C in a glass vessel under an atmosphere of  $\text{N}_2$ . This produced a solid residue and a mixture of volatile byproducts such as benzene and variable amounts of  $\text{Ph}_2\text{GeH}_2$  where the ratio of the compounds could be controlled by the reaction conditions. This result provides a proof-of-concept corroboration of the decomposition described by eq 4, and suggests that reaction kinetics can be further tuned to promote the benzene decomposition channel. We anticipate that future gas phase decomposition reactions under kinetically controlled CVD conditions will likely lead to the desired result.

We also consider a second more thermodynamically relevant reaction based on the decomposition of the compounds into conventional standard states for all of the constituent elements, as shown in eq 4, thus approximating the standard heat of formation:



In the above reactions we first computed the ground state electronic energies of the elemental Si, Ge, Sn, (diamond structures), C (graphite), and the binary phases SiSn and

(21) Baumgartner, J.; Fischer, R.; Fischer, J.; Wallner, A.; Marschner, C.; Flrke, U. *Organometallics* **2005**, *24*(26), 6450–6457.

(22) Sharma, H. K.; Cervantes-Lee, F.; Parkanyi, L.; Pannell, K. H. *Organometallics* **1995**, *15*, 429–435.

(23) Parkanyi, L.; Kalman, A.; Pannell, K.; Sharma, H. *J. Organomet. Chem.* **1994**, *484*, 153–159.

(24) Chieh, P. C.; Trotter, J. *J. Chem. Soc. A* **1970**, *6*, 911–914.

GeSn (zinc blende). We employed the VASP code<sup>25</sup> to optimize the structures using the generalized gradient approximation (GGA)<sup>26</sup> for exchange and correlation. All elements were treated using standard PAW pseudo-potentials<sup>27</sup> supplied with the package, and d-electron valence states were included for the heavier Ge and Sn. An energy cutoff of 450 eV was used in all calculations, and 80–190 irreducible  $k$ -points were used for the reciprocal space quadratures. Stringent energy convergence tolerances and expanded Fourier grids yielded optimized structures with residual atomic forces and cell stresses less than  $10^{-5}$  eV/Å and 0.001 kB, respectively. The above computational conditions yielded ground state energies:  $E[\text{C}(\text{s})] = -9.1860$  eV,  $E[\text{Si}(\text{s})] = -5.4308$  eV,  $E[\text{Ge}(\text{s})] = -4.4884$  eV,  $E[\text{Sn}(\text{s})] = -3.8033$  eV,  $E[\text{SiSn}(\text{s})] = -8.9590$  eV, and  $E[\text{GeSn}(\text{s})] = -8.2632$  eV. We note that the reference state for these energies is that of the spin-compensated neutral atom constituents.

For the gas phase reactants ( $\text{Ph}_3\text{SnSiH}_3$ ,  $\text{Ph}_3\text{SnGeH}_3$ ) and products ( $\text{H}_2$ ,  $\text{C}_6\text{H}_6$ ) the electronic energies of the optimized structures were obtained using the same computational settings as described for the solids (e.g., cutoffs,  $k$ -point grids and tolerances), but by placing the individual molecules into a large supercell of fixed edge length 10–15 Å to eliminate self-interactions between molecules. The structure of a given species is then obtained by optimizing only the atomic degrees of freedom yielding the following molecular energies:  $E[\text{Ph}_3\text{SnSiH}_3(\text{g})] = -234.5933$  eV,  $E[\text{Ph}_3\text{SnGeH}_3(\text{g})] = -233.3235$  eV,  $E[\text{H}_2(\text{g})] = -6.7845$  eV, and  $E[\text{C}_6\text{H}_6(\text{g})] = -76.0555$  eV. In the foregoing and subsequent discussions, the individual electronic energies of the molecules and solids are given in eV (96.485 kJ/mol), while energy differences (reaction energies) are given in kJ/mol.

Using the above data the reaction energies to form solid SiSn and GeSn from  $\text{Ph}_3\text{SnSiH}_3$  and  $\text{Ph}_3\text{SnGeH}_3$ , respectively, are estimated from eq 3 to be  $-244$  kJ/mol and  $-300$  kJ/mol. These large values indicate a strong tendency of both molecules to disproportionate and produce the target solids, and suggest that the driving force to form the GeSn phase from  $\text{Ph}_3\text{SnGeH}_3$  is greater than that of the Si analogue by  $\sim 0.58$  eV, or about 56 kJ/mol. Finally, the negative energy values obtained from eq 4 provide crude approximations to the heats of formation of  $\text{Ph}_3\text{SnSiH}_3$  and  $\text{Ph}_3\text{SnGeH}_3$  of +101 and +133 kJ/mol, respectively, indicating that the latter compound is slightly more stable. The relationship between the reaction energies in eq 3 and the formation heats (eq 4) is illustrated graphically in Figure 2, which shows that the energy differences between the  $\text{Ph}_3\text{SnSiH}_3$  and  $\text{Ph}_3\text{SnGeH}_3$  is larger than either that of the alloys (eq 3) or the standard state products (eq 4).

While the above data provides some basic insight into molecular stability and disproportionation reaction trends, a quantitative description of the thermochemistry requires a systematic inclusion of vibrational, rotational,

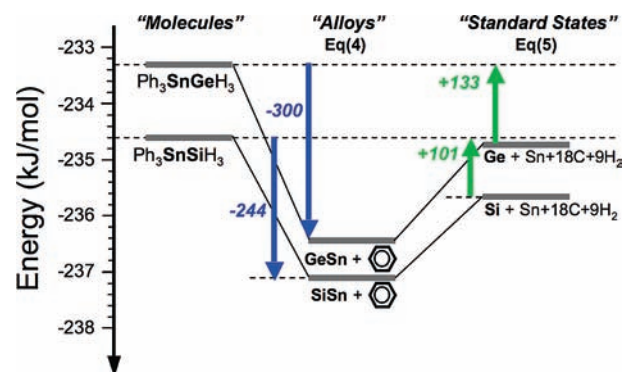


**Figure 2.** Graphical depiction of the electronic energies involved in the disproportionation and formation reactions described by eq 3 and eq 4, respectively.

and translational effects for both the gas phase and solid state systems. In the context of reactions such as those described by eq 3 and eq 4, which involve the condensation of large gas phase species into solid form, the change in zero-point energy (ZPE) represents a dominant contribution. To compute the latter for the gas phase molecules we employed the Gaussian03 code using the same DFT functional as in the VASP calculations described above, while for the solids the ZPE correction was obtained from the phonon spectrum of the ground state solids using a well-established procedure.<sup>28</sup> In particular, the dynamical matrix of the solids was calculated using special “frozen phonon” displacements in a supercell, large enough to converge the relevant interaction energies (to be described in detail elsewhere). These methodologies provided the following ZPE estimates (in kJ/mol) for the extended solid phases: Si(5.92), Ge(3.37), Sn(2.18), SiSn(8.09), GeSn(5.59), and C(graphite,6.38), while for the gas phase species we obtained:  $\text{Ph}_3\text{SnSiH}_3$ (779.8),  $\text{Ph}_3\text{SnGeH}_3$ (775.2),  $\text{C}_6\text{H}_6$ (281.6), and  $\text{H}_2$ (27.5). Combining the preceding values with the electronic reaction energies described above (Figure 2), we find ZPE-corrected disproportionation reactions energies for  $\text{Ph}_3\text{SnSiH}_3$  and  $\text{Ph}_3\text{SnGeH}_3$  to be  $-181$  kJ/mol and  $-242$  kJ/mol, respectively. The corresponding heats of formation are found to be +409 kJ/mol for  $\text{Ph}_3\text{SnSiH}_3$  and +412 kJ/mol for the Ge analogue. Perhaps not surprisingly, the latter value is quite similar to the standard heat of formation of related compounds such as tetraphenyl germanium (+445 kJ/mol) and triphenyl phenylethynyl germanium (+579 kJ/mol).<sup>29</sup> We note that the inclusion of ZPE corrections has not altered the basic trends illustrated in Figure 2; the driving force for the formation of MSn alloys is larger for the Ge compound than for its Si analogue, and the heat of formation of  $\text{Ph}_3\text{SnGeH}_3$  is predicted to be marginally larger ( $\sim 3$  kJ/mol) than that of  $\text{Ph}_3\text{SnSiH}_3$ . The optimized structures of  $\text{Ph}_3\text{SnSiH}_3$  and  $\text{Ph}_3\text{SnGeH}_3$ , including their key bond lengths and bond angles are shown in Figure 3 while Table 3 compares the measured and simulated M–Sn bond length data for the compounds with those in the corresponding SiSn and GeSn extended solids. As can be seen from the data, all simulated bond lengths are typically 1–2% larger than the experimental counterparts,

(25) (a) Kresse, G.; Furthmüller, J. *Phys. Rev. B* **1996**, *54*, 11169.

(b) Kresse, G.; Hafner, J. *J. Phys. Condens. Matter* **1992**, *6*, 8245.

(26) Perdew, J. P.; Chevary, J. A.; Vosko, S. H.; Jackson, K. A.; Pederson, M. R.; Fiolhais, C. *Phys. Rev. B* **1992**, *46*, 6671.

(27) Blochl, P. E. *Phys. Rev. B* **1994**, *50*, 17953.

(28) Atsushi, T.; Fumiyasu, O.; Tanaka, I. *Phys. Rev. B*, **2008**, *78*, 134106-1-9.

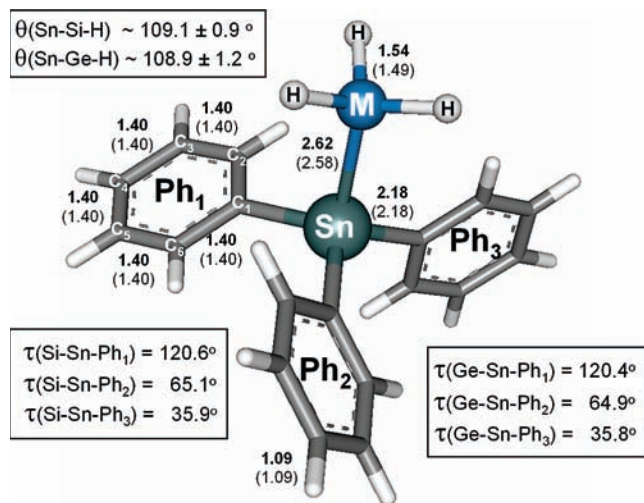


**Figure 3.** Molecular structure of  $\text{Ph}_3\text{SnMH}_3$  molecules obtained from simulation (bond lengths given in Angstrom). The primary differences occur in the Sn–M and M–H bonds, while the remaining structure including the internal structure and relative orientation of the phenyl units remains essentially unchanged (all C–C–C angles within the rings exhibit an average value of  $120.0 \pm 0.6^\circ$ ).

**Table 3.** Comparison of Observed and Calculated Values M–Sn Bond Lengths in the Title Compounds and Extended SiSn and GeSn Solid Alloys<sup>a</sup>

system	M–Sn (Å)		system	M–Sn (Å)	
	simulated	experimental		simulated	experimental
$\text{Ph}_3\text{SiSnH}_3$	2.582	2.556	SiSn	2.625	2.582
				2.599*	2.56*
$\text{Ph}_3\text{GeSnH}_3$	2.621	2.583	GeSn	2.684	2.631
				2.657*	2.61*

<sup>a</sup> The experimental values for the latter are obtained from a linear interpolation of the elemental Si, Ge and  $\alpha$ -Sn crystal structures. The values containing the asterisk represent alloy bond lengths scaled by a factor 0.99.

which is a well-known artifact of the GGA<sup>26</sup> used in DFT. Nevertheless, these data corroborate the observed trend that the M–Sn bond length in  $\text{Ph}_3\text{SnGeH}_3$  is larger than that in  $\text{Ph}_3\text{SnSiH}_3$ , as expected. We note that “experimental” Si–Sn and Ge–Sn bond lengths for the hypothetical SiSn and GeSn alloys (shown in Table 3) were deduced from the known values of the Si, Ge, and Sn diamond structures by linearly interpolating between the homonuclear bond lengths in the constituent elemental solids (Vegard’s law).

It is generally well-established that the bond length between a given pair of atoms in a regular solid are slightly dilated ( $\sim 1\%$ ) in comparison to the same bond in a molecular setting. For example, the observed Si–Si bond length 2.33 Å in disilane  $\text{Si}_2\text{H}_6$  is about 1% smaller than that in the corresponding cubic silicon structure (2.352 Å). A similar reduction in bond length is found between elemental Ge (2.45 Å) and digermane (2.41 Å). On the basis of this observation, we have included in Table 3 that the bond lengths scaled by the factor of 0.99 for the stoichiometric SiSn and GeSn alloys (indicated by asterisks) which, agree remarkably well with the observed Si–Sn and Ge–Sn bond lengths in the  $\text{Ph}_3\text{SnSiH}_3$  and  $\text{Ph}_3\text{SnGeH}_3$  molecules, respectively. Finally, we note that the same scaling and correspondence between the

molecules and solid state analogues is essentially corroborated by our simulations.

## Conclusion

We have demonstrated for the first time the synthesis of robust and air-stable  $\text{Ph}_3\text{SnSiH}_3$  and  $\text{Ph}_3\text{SnGeH}_3$  compounds containing both direct Sn–Si and Sn–Ge bonds and the typically highly reactive  $\text{GeH}_3$  and  $\text{SiH}_3$  moieties intact. We ascribe this unexpected stability in part to the crystallographic packing in the solid state structures where the latter groups are protected by encapsulating phenyl cages. The compounds were fully analyzed by chemical and spectroscopic methods to establish their elemental composition and bonding properties. XRD single crystal determination of the molecular structures revealed that the solids are isostructural. Theoretical simulations indicated that the compounds should disproportionate readily to form the corresponding SnSi and SnGe stoichiometric solids via elimination of stable  $\text{C}_6\text{H}_6$  byproducts. These experiments will be pursued as part of a comprehensive study in the near future to produce Sn-rich semiconductors. We also established experimental and theoretical correlations between the molecular Si–Sn and Ge–Sn bonds in the title compounds and those in the extended binary solids thereby providing guidance for future studies involving the development of semiconductors based on the Si–Ge–Sn optoelectronic system.

## Experimental Section

**General Considerations.** All manipulations were carried out under inert atmosphere ( $\text{N}_2$  or He) using standard high vacuum line and drybox techniques. Dry, air-free solvents were distilled from either anhydrous  $\text{CaCl}_2$  or sodium benzophenone ketyl prior to use. The NMR spectra were collected on a Varian Inova 500 MHz spectrometer. The samples were dissolved in deuterated toluene, and the  $\text{Me}_4\text{Si}$  or  $\text{Me}_4\text{Sn}$  compounds were used as an internal reference. The FTIR spectra were recorded on a Nicolet-Magna IR 550 spectrometer either as a Nujol mull between KBr plates or in a 10 cm gas cell fitted with KBr windows. Elemental analyses were performed by Columbia Analytical (Tucson, Arizona). Mass spectrometry (Direct Insertion EIMS) data were obtained using a JEOL JMS-GC Mate II spectrometer in the ASU departmental mass spectrometry facility. Lithium metal,  $\text{HSO}_3\text{C}_4\text{F}_9$ ,  $\text{PhSiCl}_3$  (Aldrich),  $\text{Ph}_3\text{SnCl}$  (Alfa Aesar), and electronic grade  $\text{GeH}_4$  gas (donated by Voltaix, Inc.) were used as received. Bromine (Alfa Aesar) was stored over  $\text{P}_2\text{O}_5$  prior to use. The starting materials triphenyltin lithium, silyl nonafluorobutanesulfonate, bromogermane, and phenylsilane were prepared according to literature procedures.<sup>18,19,30,31</sup>

**Synthesis of  $\text{Ph}_3\text{SnSiH}_3$ .** To a stirring solution of  $\text{Ph}_3\text{SnLi}$  (4.68 g, 13 mmol/35 mL THF), a stoichiometric amount of  $\text{H}_3\text{Si}(\text{SO}_3\text{C}_4\text{F}_9)$  (4.32 g, 13 mmol) was added dropwise at  $-35^\circ\text{C}$ . The reaction flask was warmed to  $23^\circ\text{C}$ , and the solution stirred for 1 h. The volatiles were removed in vacuo, and the resultant solid was extracted with dry toluene to dissolve the product and minor amounts of tetraphenyl tin. The latter impurity was precipitated out by cooling to  $-30^\circ\text{C}$  and separated from the solution via filtration. The toluene was then removed from the filtrate in vacuum to yield a white solid which was recrystallized from hexane at  $-30^\circ\text{C}$  to produce transparent

(29) Carson, A. S.; Jamea, E. H.; Laye, P. G.; Spencer, J. A. *J. Chem. Thermodyn.* **1988**, *20*, 1223–1229.

(30) Swinarski, M. F.; Onyszczuk, M. *Inorg. Synth.* **1974**, *15*, 157–161.

(31) Zech, J.; Schmidbauer, H. *Chem. Ber.* **1990**, *123*, 2087–2091.

crystals of  $\text{Ph}_3\text{SnSiH}_3$  (2.00 g, 40% yield).  $^1\text{H}$  NMR:  $\delta$  3.66 (s,  $^1J_{\text{Si-H}} = 200$  Hz,  $^2J_{\text{Sn-H}} = 56$  Hz, 3H, Si-H<sub>3</sub>),  $\delta$  7.13 (m, 9H, *m*-Ph, *p*-Ph), 7.52 (m, 6H, *o*-Ph,  $^3J_{\text{Sn-H}} = 4$  Hz).  $^{29}\text{Si}$  NMR:  $\delta$  -106.  $^{119}\text{Sn}$  NMR:  $\delta$  -133.6. Anal. Calcd for  $\text{C}_{18}\text{H}_{18}\text{SnSi}$ : C, 56.70; H, 4.76. Found: C, 56.92; H, 4.95. Mp = 86 °C. EIMS (*m/e*): isotopic envelope centered at 351 ( $\text{M}^+ - \text{SiH}_3$ ). IR (film,  $\text{cm}^{-1}$ ): 3135 (vw), 3066 (w), 3047 (w), 3020 (w), 3002 (w), 2164 (s), 2130 (s), 1955 (w), 1883 (w), 1852 (w), 1769 (vw), 1640 (vw), 1579 (w), 1479 (s), 1429 (vs), 1376 (w), 1331 (m), 1301 (m), 1262 (w), 1192 (vw), 1156 (vw), 1072 (s), 1022 (m), 999 (m), 973 (vw), 918 (m), 845 (vs), 729 (vs), 697 (vs) 453 (s), 439 (s), 314 (m).

**Synthesis of  $\text{Ph}_3\text{SnGeH}_3$ .**  $\text{BrGeH}_3$  (1.70 g, 11 mmol) was condensed at -196 °C into a 100 mL Schlenk flask containing a THF solution of  $\text{Ph}_3\text{SnLi}$  (4.1 g, 11 mmol/50 mL THF). The flask was first warmed to -40 °C and stirred for 1 h at this temperature to produce a dark solution. The latter was then warmed to room temperature and stirred for an additional 14 h after which the volatiles were removed in vacuo to leave behind a white solid. This was extracted with toluene to dissolve the product and minor amounts of tetraphenyl tin impurity. Crystalline  $\text{Ph}_3\text{SnGeH}_3$  was obtained (2.40 g, 50% yield) following the same procedure described above for the  $\text{Ph}_3\text{SnSiH}_3$  analogue:  $^1\text{H}$  NMR:  $\delta$  3.50 (s,  $^2J_{\text{Sn-H}} = 82$  Hz, 3H, Ge-H<sub>3</sub>),  $\delta$  7.11 (m, 9H, *m*-Ph, *p*-Ph), 7.49 (m, 6H, *o*-Ph).  $^{119}\text{Sn}$  NMR:  $\delta$  -134.2. Anal. Calcd for  $\text{C}_{18}\text{H}_{18}\text{SnGe}$ : C, 50.77; H, 4.26. Found: C, 50.63; H, 4.27. Mp = 82 °C. EIMS (*m/e*): isotopic envelope centered at 426 ( $\text{M}^+$ ). IR (film,  $\text{cm}^{-1}$ ): 3135 (vw), 3066 (w), 3047 (w), 3016 (vw), 2080 (s), 2045 (s), 1960 (w), 1880 (vw), 1830 (vw), 1769 (vw), 1644 (vw), 1581 (w), 1482 (m), 1431 (s), 1381 (vw), 1336 (m), 1301 (m), 1262 (w), 1195 (vw), 1162 (vw), 1077 (s), 1027 (m), 1002 (m), 888 (w, br), 778 (vs), 733 (vs), 703 (vs) 455 (s).

**X-ray Structure of  $\text{Ph}_3\text{SnSiH}_3$  and  $\text{Ph}_3\text{SnGeH}_3$ .** Colorless crystalline blocks of  $\text{Ph}_3\text{SnSiH}_3$  (0.34 mm × 0.34 mm × 0.22 mm) and  $\text{Ph}_3\text{SnGeH}_3$  (0.27 mm × 0.21 mm × 0.15 mm) were mounted on glass fibers using Apiezon grease for subsequent data collection. The data for both compounds were collected at 123 K using Bruker APEX type diffractometers

and associated software.<sup>32,33</sup> Three sets of 606 frames (0.3 wide in  $\omega$  with 10 s exposure) were taken at  $\varphi = 0^\circ$ ,  $120^\circ$ , and  $240^\circ$  for both materials. The resulting 1818 frames for each compound were then integrated (SAINT) and corrected for absorption (SADABS). This procedure produced 6935 and 6689 measured reflections for  $\text{Ph}_3\text{SnSiH}_3$  and  $\text{Ph}_3\text{SnGeH}_3$ , respectively. The space group was determined to be  $P\bar{1}$  (triclinic, No. 2) for both materials using the XPREP module contained in SHELXTL, giving 3014 and 3030 unique reflections for  $\text{Ph}_3\text{SnSiH}_3$  and  $\text{Ph}_3\text{SnGeH}_3$ , respectively. Both structures were solved using standard runs of XS and refined using XL. After an initial refinement of the anisotropic thermal parameters for the heavy atoms, the hydrogens were then added geometrically to the phenyl groups. Subsequent refinement produced peaks in the Fourier difference map at expected positions and electron densities for the H atoms of the SiH<sub>3</sub> group of  $\text{Ph}_3\text{SnSiH}_3$ . The positions and isotropic thermal parameters of the latter were then included in the refinement parameters resulting in a final R1-value of 0.0251 for 193 parameters and 2912 reflections having  $I_{\text{obs}} \geq 2\sigma(I)$ . For the  $\text{Ph}_3\text{SnGeH}_3$  compound the analogous H peaks were not visible in the difference map about the Ge atom. In this case hydrogen atoms were simply added geometrically and allowed to refine as a rotating rigid group at a fixed distance of 1.55 Å from Ge, resulting in the final R1-value of 0.0418 for 182 parameters and 2710 reflections having  $I_{\text{obs}} \geq 2\sigma(I)$ .

**Acknowledgment.** This research was supported by the U.S. Air Force Office of Scientific Research (AFOSR MURI, FA9550-06-01-0442), Voltaix Corporation, and NSF (IIP 075049).

**Supporting Information Available:** Crystallographic data for  $\text{Ph}_3\text{SnSiH}_3$  and  $\text{Ph}_3\text{SnGeH}_3$  (CIF). This material is available free of charge via the Internet at <http://pubs.acs.org>.

(32) SMART (Version 5.632), SAINT (Version 6.45a), SHELXTL (Version 6.14), and SADABS (Version 2.10); Bruker AXS Inc.: Madison, WI, 2003.

(33) APEX2 (Version 2009.1-0), SAINT (Version 7.60a), SHELXTL (Version 2008/4), and SADABS (Version 2008/1); Bruker AXS Inc.: Madison, WI, 2009.